Presented at the 23rd European Photovoltaic Solar Energy Conference, Valencia, Spain, 1-5 September 2008

COST & EFFICIENCY OPTIMISATION OF THE FLUORESCENT SOLAR CONCENTRATOR

E.E. Bende[1], L.H. Slooff[1], A.R. Burgers[1], W.G.J.H.M. van Sark[2], M. Kennedy[3]
[1]ECN Solar Energy, P.O. Box 1, 1755 ZG Petten, The Netherlands
[2]University of Utrecht, The Netherlands
[3]Dublin Institute of Technology, Ireland
Tel: +31 224 56 4122, Fax: +31 224 56 8241, Email: bende@ecn.nl

ABSTRACT:
The Fluorescent[1] Solar Concentrator (FSC) is a polymer plate that contains a fluorescent species and that has photovoltaic (PV) cells attached to its small sides. Light that impinges on the plate is absorbed and subsequently emitted by the fluorescent material. Part of the emitted light is subject to total internal reflection and eventually strikes on the PV cells. When a (square) FSC gets longer, both its efficiency and cost decrease. The efficiency decrease can be ascribed to increasing losses due to self-absorption and back-ground absorption. The cost decrease can be attributed to an increasing ratio of the area of the relatively cheap polymer plate to that of the expensive PV cells. These two trends combined lead to a minimum in the cost-per-unit-of-power at a certain size. In this work, we compute both cost [€/m^2] and power per unit area [W/m^2] as well as the cost-per-unit-of-power [€/W] on the basis of a simple cost model and by simulations using a ray-tracing program. We perform a parameter study and find the optimal FSC. Adopting from another study, a cost-per-unit-area ratio of the polymer plate-to-PV of 1:15, we calculate a cost-per-unit-of-power that is only 35% of that of conventional PV. We identify enhancement possibilities of the device and present the corresponding cost-per-unit-of-power reductions. Moreover, we present results of an FSC with an optimized Cholesteric Top Mirror (CTM) and show that a relative gain in efficiency of 14% is possible.
Keywords: Fluorescent solar concentrator, Luminescent solar concentrator, Cost optimization

1 INTRODUCTION

Due to the high prices of conventional crystalline-Si photovoltaic cells (PV-cell) alternatives are sought that require less of the expensive silicon and are therefore capable of converting light into electricity at lower costs. One of the alternatives is the Fluorescent Solar Concentrator (FSC).

The FSC consists of a transparent plate with solar cells attached to one or more sides. The plate contains a fluorescent material like an organic dye (or an amount of quantum dots) which absorbs the incident sun light within a certain wavelength range and subsequently emits it isotropically at higher wavelengths. A fraction of the emitted light undergoes total internal reflection (TIR) and eventually reaches the PV cell(s) as depicted by ray number nine in Figure 1. TIR takes place when the ray hits the surface at an angle with the surface normal, θ, that is bigger than the critical angle ($\theta > \theta_{cr}$). The latter is determined by Snell's law and reads θ_{cr}=arcsin (1/n) in which n is the refractive index of the polymer plate.

A cost reduction is realized when the area of the expensive PV cells is small compared to the top area of the relatively cheap polymer plate.

Referring to the rays in Figure 1 we can identify the following loss mechanisms in an FSC: Incident light traverses back and forth through the plate since no absorption takes place (1), incident light is absorbed by the non-ideal mirror (2), incident light is absorbed by the polymer (3), light is absorbed and subsequently emitted by the dye within the escape cone ($\theta < \theta_{cr}$) thus leaving the FSC (4), incident light is absorbed by the dye and subsequently not emitted due to the dye's less-than-unity quantum efficiency (QE) (5), emitted light is absorbed by the polymer (6), emitted light is absorbed by the mirror (7) and, lastly, light emitted by the dye is reabsorbed by the dye (i.e. self absorption) and re-emitted within the escape cone (8).

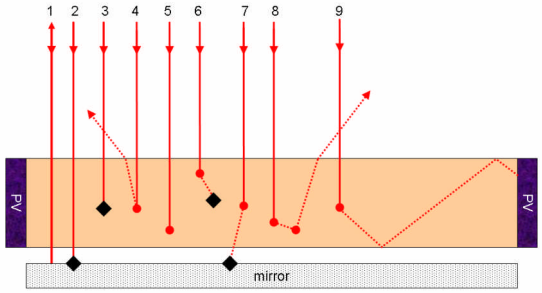

Figure 1 Schematic presentation of the FSC showing the destinies of incident light rays (solid) and emitted light (dashed). The circles represent absorption by the fluorescent and the black diamonds represent parasitic absorption by the polymer or mirror. Rays 1 to 8 represent losses, whereas ray 9 shows the desired behavior of light emitted by the fluorescent, undergoing total internal reflection and reaching a PV cell at one of the sides of the plate.

Although an FSC suffers from these losses, it also has some characteristic advantages. Due to the high top-to-side area ratio of the polymer plate the light is concentrated at the sides. Shockley's diode equation tells us that the open-circuit voltage (V_{oc}) is linear in ln(j_{sc}), where j_{sc} is the shortcut current-density which is proportional to the light intensity. The fill-factor increases on its turn with increasing V_{oc} (see section 5.4.4 of [1]). The PV-cell is small and therefore has short

[1] Throughout this paper we use the term "fluorescent" rather than the often-used term "luminescent", since the former is a special case of the latter, and hence describes the process more directly.

fingers resulting in low series resistance, implying an even higher fill factor. In addition to that, figure 1 shows that for some fluorescent species light is emitted in the wavelength range where the PV-cell's internal quantum efficiency is close to unity. These effects lead to a high efficiency of the PV-cell within the FSC. Clearly, these positive effects and the loss mechanisms together determine the over-all efficiency of the FSC.

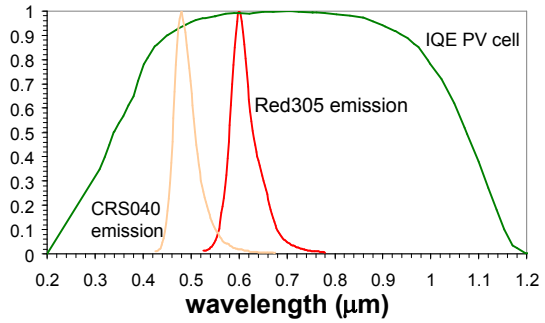

Figure 2 The internal quantum efficiency of the PV cell and the emission spectra of the dyes used in this study. Note that the Red305 peak emission occurs at an IQE of unity, whereas the CRS040 occurs at sub-unity.

For electricity generation the concept of the FSC is viable if the electricity costs expressed in €/W are lower than that of conventional PV. This can only be the case if the area costs of the polymer plate in €/m^2 are sufficiently low compared to that of the PV cells.

In this study, we have carried out a comprehensive parameter study to assess the performance of the FSC on the basis of simulations. We calculate the relative costs, i.e. compared to conventional PV, in $(€/m^2)_{FSC}/(€/m^2)_{PV}$ and the relative power in $(W/m^2)_{FSC}/(W/m^2)_{PV}$, as a function of the system parameters. This approach was adopted from [2].

2 FSC-MODEL

In this work, we consider an FSC module that can be thought of as an infinite chess board, where every square represents a polymer plate and where the interfaces between the squares represent bifacial solar cells (e.g. see [4] & [5]). Figure 3 shows one unit-cell of such a module. For this configuration, two PV cells, on average, belong to one square polymer plate.

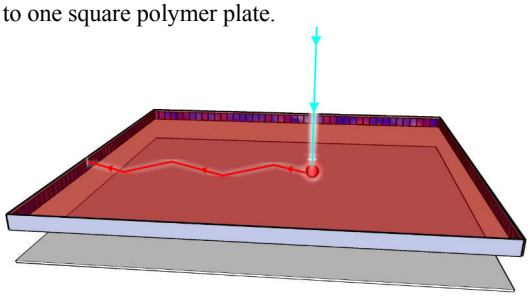

Figure 3 One square of the "chess board" FSC module. The square is surrounded by four PV-cells. Below the polymer plate a bottom mirror with air gap is visible.

In the simulation, we model only one square that has four attached solar cells. For the fluorescent, we considered a mixture of Lumogen F Red 305 from BASF (Red305) and CRS 040 (Crs040) from Radiant Color. Figure 2 shows their absorption cross sections and emission spectra. Furthermore, in the model we used the following (observed) physical parameters. The polymer plate has a refractive index n of 1.49, the back-ground absorption coefficient of the polymer plate is 1 m^{-1}. Both dyes have quantum efficiencies of 0.95, which implies that per absorbed photon 0.95 photons are emitted on average. The bottom mirror, if present, has a constant reflectivity of 0.98.

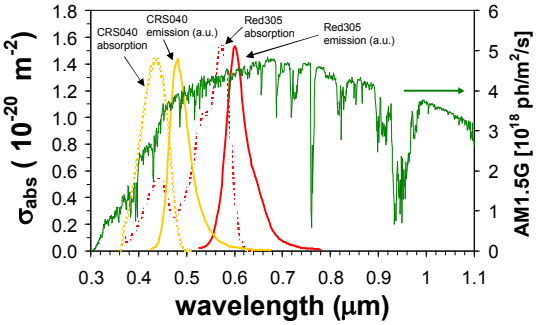

Figure 4 Absorption cross section and emission spectra (a.u.) for Crs040 Yellow and Red305 as well as the AM1.5G spectrum [photons/m^2/s].

2.1 Simulation

We simulate the behavior of the FSC with an in-house built computer program [3]. This program is a ray-trace program based on Monte Carlo techniques.

Random numbers are drawn to simulate the faith of the photon. Based on Beer's law (exponential) weighted distribution, a random number is used to determine the traversal length of a photon. Furthermore, random numbers are used to determine the type of absorption (dye or polymer), the emission/no-emission event by the dye (based on the quantum efficiency), the direction of isotropically emitted light (independently of the direction of incident light), the wavelength of emitted light as well as the transmission/reflection choice at the interfaces of the plate (based on reflection coefficients).

The polymer-PV reflection coefficients are determined by converting the air-PV reflection coefficients with the help of the Fresnel equations.

2.2 Parameter study

We perform a parameter study with the following parameters: The (square) polymer plate length (l), its thickness (d), the total concentration of the two dyes (C), the fraction of CRS040 Yellow (f) and that of CRS Red305 (1-f) as well as the bottom-mirror configuration. The latter can be one of the following:

1. Specular with air gap (between plate and mirror).
2. Lambertian with air gap.
3. Lambertian without air gap
4. No bottom mirror.

The specular mirror without airgap has been disregarded since previous studies [6] have shown that this always yields worse performance compared to one with air gap.

2.3 Constraints

During the calculation the following constraints for the parameters have been imposed:

1. $0.001 \le d \le 0.01$ [m]
2. $d \le l \le 10$ [m]
3. $5.62 \cdot 10^{20} \le C \le 5.62 \cdot 10^{24}$ [m^{-3}]
4. $0 \le f \le 1$

The maximum constraint for the concentration is set to prevent so-called concentration quenching [7], which takes place when the distance between the dye molecules becomes too low, and which leads to a drop in quantum efficiency.

3 OPTIMIZATION CONCEPT

3.1 Introduction

The most important properties of the FSC are obviously its costs per unit area and its power per unit area. Since we are comparing an FSC with conventional PV we will express these quantities as a fraction of their conventional counterparts. Hence, we will use the dimensionless quantities C_r for relative cost in $(€/m^2)_{FSC}/(€/m^2)_{PV}$ and P_r for the relative power density in $(W/m^2)_{FSC}/(W/m^2)_{PV}$. For electricity generation one is inclined to minimize the ratio C_r/P_r, for this results in the lowest relative cost-per-unit-of-power in $(€/W)_{FSC}/(€/W)_{PV}$. However, the question is if this really is what someone is aiming for. Table 1 shows hypothetical FSC's. System 1 has a cost-per-unit-of-power is twice as low as that of conventional PV (i.e. $C_r/P_r=0.5$), but its relative power, and hence its efficiency, is only one tenth (i.e. $P_r=0.1$). In that case, one has a system with 'cheap' power, but with hardly any output. Maybe one might prefer system 2 that has slightly higher cost-per-unit-of-power but with substantially higher output, e.g. $C_r/P_r=0.55$ and $P_r=0.4$.

3.1 Target functions

With these examples we arrive at the heart of what optimization is really about. In contrast with maximization (or minimization), optimization is about finding the optimal combination of two or more objectives. This is by definition a subjective matter, since it depends on the perception of the buyer/user/producer what is felt as a good balance. In order to treat optimization in a quantitative sense, we can introduce a so-called target or objective function. Constructing a single aggregate objective function (AOF) is perhaps the most intuitive approach to solving the multi-objective problem. In case of an AOF that is the weighted linear sum of the objectives, one specifies scalar weights for each objective to be optimized. Clearly, the solution obtained will depend on the (relative) values of the weights specified. Equation 1 shows some weighted-linear-sum target functions (I-IV) as well as a novel, function (V), proposed for the first time in this work.

$$
\begin{aligned}
&\text{I.} \quad f(C_r, P_r) = aC_r + bP_r && (a \le 0, b \ge 0)\\
&\text{II.} \quad f(C_r, P_r) = aC_r + c\frac{C_r}{P_r} && (a, c \le 0)\\
&\text{III.} \quad f(C_r, P_r) = bP_r + c\frac{C_r}{P_r} && (c \le 0, b \ge 0)\\
&\text{IV.} \quad f(C_r, P_r) = aC_r + bP_r + c\frac{C_r}{P_r} && (a, c \le 0, b \ge 0)\\
&\text{V.} \quad f_\gamma(C_r, P_r) = P_r^{\gamma} / C_r^{1-\gamma} && (0 \le \gamma \le 1)
\end{aligned}
\qquad (1)
$$

It is clear that the first function allows the special cases of cost minimization ($a<0$, $b=0$) and power maximization ($a=0$, $b>0$). However, it lacks the possibility to minimize cost-per-unit-of-power as a subset of the optimization. The second function does have this possibility when $a=0$, but then power maximization is out of scope. The third function allows cost-per-unit-of-power minimization ($c<0$ and $b=0$), but disallows cost minimization. The fourth function allows all aforementioned possibilities for a proper choice of the parameters. Function V is constructed such that it also has these possibilities, but with only one parameter. For this function, the cases of power maximization, cost minimization and cost-per-unit-of-power minimization correspond with $\gamma=1$, $\gamma=0$ and $\gamma=½$, respectively. Due to its simplicity, we prefer this function and will henceforth use it.

3.1 Maximizing an example target function

We now apply the above concept to the example previously mentioned. Suppose our aim is to attain the lowest cost-per-unit-of-power. In that case we need to maximize the target function with $\gamma=½$. Table 1 shows that in that case system 1 is optimal, since it yields the maximal $f_{½}(C_r,P_r)$. However, if one is interested in a system where a 'good' trade-off between a low cost-per-unit-of-power ($\gamma=½$) and high power, i.e. high efficiency, ($\gamma=1$) occurs one could try to optimize the target function where γ lies somewhere between half and unity. So we can consider, say, $f_{¾}(C_r,P_r)$ as an appropriate target function. Table 1 shows that for that choice, system 2 is the optimal one. This system indeed has a much higher power, and thus efficiency, at the expense of only a modest increase of the cost-per-unit-of-power.

Table 1 Values of the target function $f_\gamma(C_r,P_r)$ for different choices of the parameter γ. System 1 and 2 are two hypothetical systems.

	Cr	Pr	Cr/Pr	$f_{1/2}(C_r,P_r)$	$f_{3/4}(C_r,P_r)$
System 1	0.05	0.10	0.50	1.41	0.38
System 2	0.22	0.40	0.55	1.35	0.73

Appendix A explains in detail how the quantities C_r and P_r can be calculated for an FSC.

4 COMPUTATIONAL RESULTS

In the preceding section we discussed the target function for optimization. Before discussing the integral results for that, we will discuss the three special cases, i.e. power maximization ($\gamma=1$), cost minimization ($\gamma=0$) and cost-per-unit-of-power minimization ($\gamma=½$). In addition we will focus on the effect of the dye concentrations.

4.1 Power-density maximization ($\gamma=1$).

Firstly, it should be noted that power-density maximization refers to the power per unit of *top* area of the FSC. Secondly, the power density is proportional to efficiency. To achieve the maximum power density and thus the highest efficiency the results are quite clear. Figure 5 shows the average EQE, which is the average number of electrons generated per incident photon on the top area of the FSC. From this figure one can see that the average EQE decreases with increasing length and with

decreasing thickness.

At small FSC lengths, say at 1 cm, the EQE of the thick plate is twice as high as that of the thin plate. The explanation for this is twofold. Firstly, with increasing thickness more incident photons will be absorbed. Secondly, photons that are emitted by the dye in the escape cone towards the top area might strike on the small side of the polymer plate. Obviously this effect dominates in the neighborhood of the plate's sides. If there were a polymer-air interface at the side, the photons would be subject to internal reflection and would still leave the polymer plate at the top area after reflection. However, since the edge is a polymer-PV interface the photons will now be refracted from the low-index (polymer) to a high-index medium (PV cell). This effect is much stronger, in relative sense, for small and thick polymer plates.

At larger FSC lengths the described geometrical effect becomes of less importance since the side-to-top surface ratio decreases. Then, only the increased absorption with increasing thickness is visible. At a plate length of 1 m, in combination with the max. Red305 concentration, the plate of 1 cm thickness has an average EQE that is only 8% bigger than that of its 1 mm counterpart.

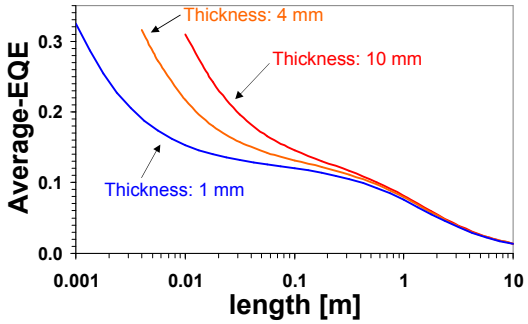

Figure 5 Average EQE for the FSC as a function of the plate length, with the thickness as a parameter (Maximum Red305 concentration, no CRS040, Lambertian bottom mirror with air gap). The average EQE represents the number of generated electrons in the FSC per incident photon.

The average EQE is proportional to the aggregated shortcut currents of the PV cells at the plate's side. Clearly, current and voltage *together* determine the power-density of the device. As mentioned in the introduction, the open-circuit voltage (V_{oc}) is linear with the logarithm of the cell's current density. Figure 6 shows that the current density increases with increasing FSC length and with decreasing thickness. At an FSC length of ~20 cm and a thickness 1 cm, the PV-cell's current density is equal to that of a bare PV cell at one sun. However, the same plate but with a thickness of only 1 mm shows a current density that is one order of magnitude greater.

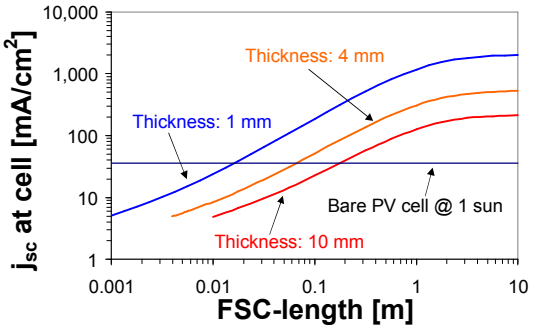

Figure 6 The short-circuit current density at the PV cell as a function of the FSC length, with the FSC thickness as a parameter (Maximum Red305 concentration, no CRS040, Lambertian bottom mirror with air gap). The horizontal line is the reference of the bare PV cell at one sun.

As a consequence of these high current densities, higher open-circuit voltages are obtained. This is shown in Figure 7.

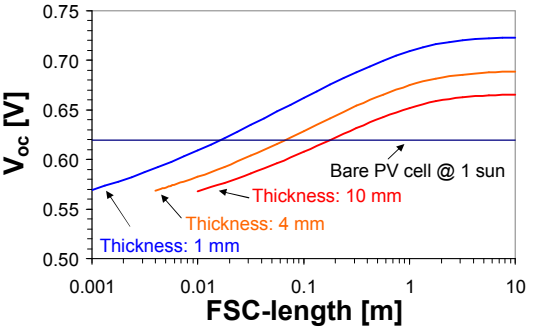

Figure 7 The open-circuit voltage as a function of the FSC length, with the thickness as a parameter (Maximum Red305 concentration, no CRS040, Lambertian bottom mirror with air gap). The horizontal line is the V_{oc} of the bare PV-cell under one sun illumination.

By combining the trends of the EQE (~I_{sc}) of Figure 5, those of the Voc (Figure 7) and the fill factor, one can calculate the FSC's power density and, therefore, its efficiency (see Appendix).

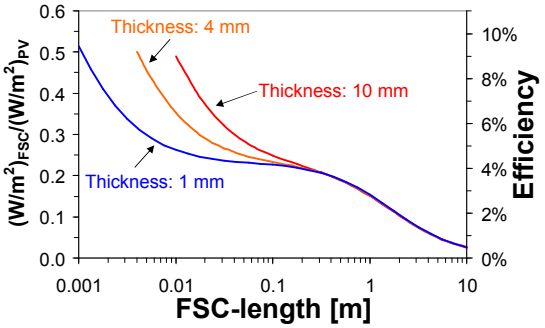

Figure 8 The relative power density (left axis) and corresponding efficiency (right axis) as a function of the FSC length, with the plate thickness as a parameter. (Maximum Red305 concentration, no CRS040 Yellow, Lambertian bottom mirror with air gap).

At large FSC lengths, the effect of the increasing EQE with increasing thickness is counterbalanced by a decreasing Voc. Figure 8 shows that at lengths of >30 cm

the relative power density curves nearly coincide. Note that in this regime a thicker plate and correspondingly wider cells would only add to the costs, whereas no efficiency gain will be obtained.

As far as power (or efficiency) maximization (γ=1 case) is concerned, Figure 8 shows that for a fixed length the highest power density is obtained for the thickest plate. Conversely, for a fixed thickness, the maximum power occurs at minimum length. However, in the entire parameter space, the maximum power is found at both minimum thickness (1 mm) and minimum length (1 mm). It is useful to realize that the PV area of such an FSC is twice as high as that of a bare PV cell, whereas its power is only one half its conventional counter part. Apart from the questionable manufacturability of such a device, this configuration is by no means a viable alternative to conventional PV. This also illustrates that high FSC efficiencies published in literature should preferably be judged in the context of their costs.

4.2 Cost minimization (γ=0).

Appendix A elaborates on the cost and power calculation performed for this work. For the calculation we have assumed that the polymer-plate to PV area-cost fraction reads C_{PP}[€/m^2] / C_{PV}[€/m^2] = 1/15. This means that the cost per unit area of the polymer plate (including the dye) is one fifteenth of that of a PV-cell. Current investigations show that this seems a realistic value [8]. Equation 4 of appendix A shows that the costs decrease with decreasing side-to-top area ratio. Furthermore, it can be seen that in the limit d / l→0, i.e. thin and long plates, the FSC-to-PV area cost ratio tends to the polymer-plate-to-PV area cost ratio, i.e. C_{PP}[€/m^2] / C_{PV}[€/m^2].

4.3 Cost-per-unit-of-power minimization (γ=½).

The preceding sections reported that both P_r and C_r decrease with increasing length, keeping other parameters fixed. However, the ratio C_r/P_r, i.e. the relative cost-per-unit-of-power, shows a minimum. Figure 9 shows that the minimal C_r/P_r occurs at about 25 cm (Lambertian mirror with air gap, d=1 mm, no CRS040, max. Red305 concentration). For this configuration C_r/P_r=0.35, which implies that the FSC can generate power at a cost price that is only 35% of that of conventional PV, in terms of €/W. In this work we discard the cost-per-unit-of-energy [€/kWh], since this is hard to calculate as it involves uncertainties with regard to the lifetime of the device and in particular that of the dyes. However, recent life-time experiments for a Red305-plate [9] show promising results in that respect: Only 3% degradation, after 85 weeks of outdoor illumination.

When the plate gets thicker the minimum shifts to higher lengths (l=56 cm for d=1 cm) and becomes higher, namely C_r/P_r=0.56.

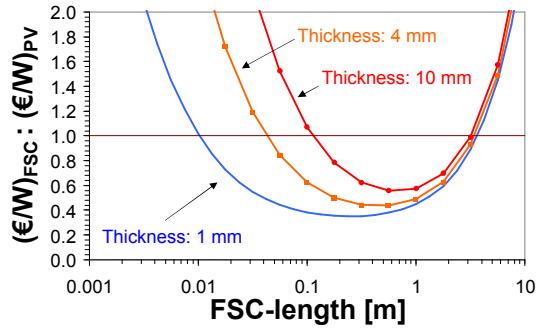

Figure 9 Relative cost-per-unit-of-power [(€/W)$_{FSC}$ /(€/W)$_{PV}$] as a function of the FSC length, with the thickness as a parameter. (Polymer-plate to PV cost per unit of area fraction, C_{PP}[€/m^2] / C_{PV}[€/m^2] = 1/15, maximum Red305 concentration, no CRS040 Yellow, Lambertian bottom mirror with air gap)

As mentioned before the polymer-plate to PV cost-per-unit-area is the key parameter in the cost-per-unit-of-power minimization. Since this number is quite sensitive to assumptions in a detailed cost model it is useful to assess the cost-per-unit-of-power for a range of values. Figure 10 shows the optimal relative cost-per-unit-of-power (C_r/P_r) as a function of C_{PP}[€/m^2] / C_{PV}[€/m^2], as well as the corrseponding optimal FSC length.

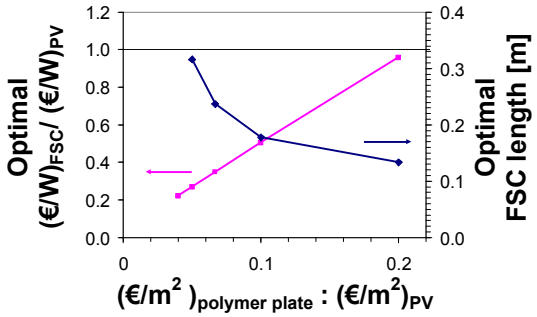

Figure 10 The optimal relative cost-per-unit-of-power (C_r/P_r , pink line) as a function of the polymer-plate-to-PV cost-per-unit-area ratio, C_{PP}[€/m^2] / C_{PV}[€/m^2], as well as the corrsponding optimal FSC length (blue line). The horizontal line represents the case where the cost-per-unit-of-power of the FSC equals that of conventional PV. All optima are found for: d=1 mm, max. Red305 concentration, no CRS040, Lambertian bottom mirror with air gap.

A fit on these data yields the following formula:

$$\left(C_r / P_r\right)_{opt} = 0.044 + 4.6 \cdot \frac{C_{PP}[€/\mathrm{m}^2]}{C_{PV}[€/\mathrm{m}^2]}. \qquad 2)$$

Both Figure 10 and eq. 2 tell us that the FSC under investigation can only give a lower cost-per-unit-of-power than conventional PV, i.e. C_r/P_r < 1, if the cost-per-unit-area of the polymer plate is more than 5 times less than that of conventional PV, i.e. C_{PP}[€/m^2]/C_{PV}[€/m^2] < 0.2. However, one should not that if C_{PP}[€/m^2]/C_{PV}[€/m^2] = 0.2, one would always prefer conventional PV since this gives a much higher power density than conventional PV. In other words, C_{PP}/C_{PV} should be well below 0.2 in order to make an FSC a viable alternative for conventional PV.

4.4 Optimal dye concentrations

Figure 4 shows that the fraction of incident photons that are converted to charge carriers (average EQE) is maximal when the total dye concentration equals the upper boundary of $5.62 \cdot 10^{24}$ m^{-3} and the Yellow CRS040 fraction is nil. An increase of the dye concentration leads on the one hand to an increase of absorption of the incident photons and on the other hand to an increase of self absorption. Self absorption obviously leads to losses due to non-unity quantum efficiency and top losses. In the regime of a total dye concentration $< 5.62 \cdot 10^{24}$ m^{-3} the former effect outweighs the latter. An increase of the fraction of CRS040 at constant total dye concentration leads to a decrease of the average EQE. This can be ascribed to the less favorable optical properties of the yellow dye CRS040. Firstly, Figure 4 shows that its absorption range is much smaller than that of the Red305 and that its shape and position is less favorable in relation to the AM1.5G spectrum. Secondly, Figure 2 shows that the emission spectrum of CRS040 yellow is less favorable compared to that of Red305, since it overlaps more with the off-unity wing of the PV cell's IQE.

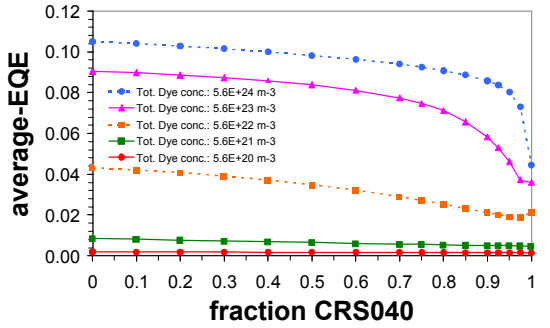

Figure 11 The fraction of incident photons converted to electrons at the four sides of the square FSC as a function of the fraction of CRS040 Yellow, with the total dye concentration as parameter (l=23.7 cm, d=1 mm).

5 OPTIMIZATION RESULTS

In the previous section we focused on three special cases of the objective function, namely γ=0, ½ and 1. In this section, we will assess the entire range $0 \le \gamma \le 1$. Figure 12 depicts the cost, the power density and the cost-per-unit-of-power, all relative to conventional PV, as a function of γ. It can be seen that the minimum cost-per-unit-of-power can indeed be found at γ=½.

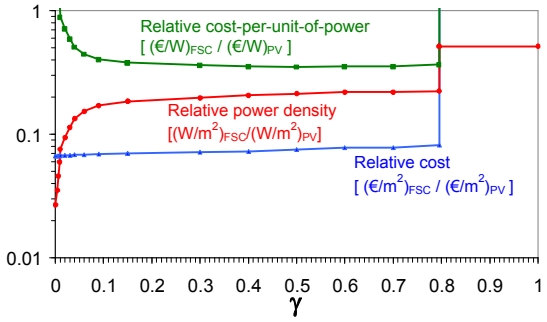

Figure 12 Multiple objectives as a function of the target function's parameter γ. Note the following special cases: minimum costs (γ=0), minimum cost-per-unit-of-power (γ=½) and maximum relative power (and thus the efficiency) (γ=1).

Furthermore, the curves of Figure 12 show a discontinuity at γ=0.795. Crossing this point causes the optimal configuration to jump from an LSC length of 13 cm to 1 mm, as can be seen from Table 2. Clearly, this jump involves a relative cost-per-unit-of-power > 1 while the relative power remains below unity, which implies that for γ>0.795 one would always prefer conventional PV.

In addition, Table 2 shows that if one chooses γ=½ (orange row) one gets the lowest cost-per-unit-of-power, which can be denoted as the classical optimization case. However, if one chooses γ=0.6 instead, one favors more power at the expensive of somewhat higher costs. In that case, the power increases by about 3% whereas the cost-per-unit-of-power increases by only 1%.

Table 2 The configuration for which the target function $f_\gamma(C_r,P_r) = P_r^\gamma / C_r^{1-\gamma}$ is maximal, listed against its parameter γ, with the following special cases: Cost minimization (γ=0, green), cost-per-unit-of-power minimization (γ=0.5, orange) and power maximization (γ=1, blue). For all γ's the following optimal parameters were found: d=1 mm, Red305 = $5.6 \cdot 10^{24}$ m^{-3}, CRS040 = 0 m^{-3} and mirror configuration: Lambertian with air gap.

γ	length [m]	Cost *relative*	Power *relative*	Cost per unit of power *relative*	η_{FSC}
0.000	10.0000	0.067	0.027	2.487	0.49%
0.009	4.2170	0.067	0.060	1.126	1.10%
0.090	0.7499	0.069	0.171	0.405	3.14%
0.150	0.5623	0.070	0.185	0.380	3.40%
0.300	0.4217	0.071	0.197	0.362	3.62%
0.500	0.2371	0.075	0.213	0.352	3.92%
0.600	0.1778	0.078	0.219	0.356	4.03%
0.794	0.1334	0.082	0.224	0.365	4.11%
0.795	0.0010	2.067	0.514	4.019	9.45%
1.000	0.0010	2.067	0.514	4.019	9.45%

5 FURTHER IMPROVEMENTS

5.1 Changing model parameters

In order to identify to what extent the FSC can be improved we performed ray-trace computations for the following improvements:

1. An increase of the refractive index of the polymer plate from 1.5 to 1.7 to reduce the escape cone losses ("N+0.2") .
2. A shift of +50 nm of the emission spectrum to reduce self absorption ("stokes +50nm").
3. A reduction of the polymer absorption from 1 to 0.1 m^{-1} ("alpha=0.1").
4. An increase of the Red305 quantum efficiency from 0.95 to 1 ("q=1").
5. All of the preceding improvements together ("N+0.2,stokes+50nm,alpha=0.1,q=1").

Figure 13 and Figure **14** show the corresponding power and cost-per-unit-of-power curves. As can be seen all cases lead to an enhancement of both power and cost-per-unit-of-power. (Note that the cost model remained unchanged).

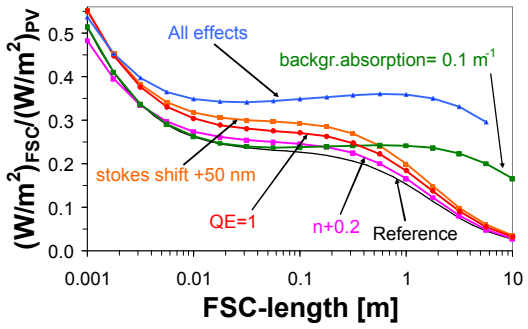

Figure 13 Relative power as a function of the FSC length for different changes. The black line is the reference case.

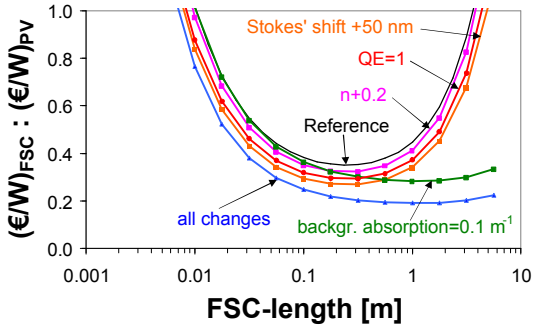

Figure 14 Relative cost-per-unit-of-power as a function of the FSC length. The black line is the reference.

It can be seen that the case of the back-ground absorption reduction ("alpha=0.1") leads to a shift of the optimal length from 25 cm to 1 m. This also comes into expression in the case that includes all improvements.

Table 3 shows the mentioned improvements and their corresponding changes in relative cost-per-unit-of-power:

Table 3 Improvement results

	Cr/Pr	Gain
reference	0.35	-
N+0.2	0.32	9%
Stokes+50 nm	0.27	23%
Alpha=0.1	0.28	20%
Q=1	0.29	17%
All changes	0.19	46%

5.2 Cholesteric top mirror

In order to reduce the top losses of an FSC one can apply a selective top-mirror. The ideal mirror is as transparent as possible for incident light and as reflective as possible for emitted light that leaves the FSC through the top escape cone. One of the candidates for such a mirror is the cholesteric top mirror (CTM).

Figure 15 shows the measured transmission spectrum of such a CTM. As can be seen this CTM has a ~90% reflectance in the 500-700 nm range that is dependent on the angle of incident light.

In this study, we modeled an FSC with the following properties: 150 nm reflection band width and 96% transmission outside the reflection band. The reflection band was modeled as a square well. The center wave length of the reflection band obeys

$$\lambda(\vartheta_0) = \lambda_0 \cos\left(\arcsin\left(\frac{n_0 \sin(\vartheta_0)}{n_2}\right)\right), \qquad 3)$$

where λ_0 is the center wavelength that depends on the angle on incidence ϑ_0 and n_0, n_2 the refractive indices for air and the polymer plate.

Figure 16 shows the relative power of the FSC, optimized for the lowest cost-per-unit-of-power, as a function of the short-wavelength edge of the band of the CTM. The short-wavelength edge equals the center wavelength minus half of the bandwidth, i.e. $\lambda_0 - ½ \cdot 150$ nm. One would expect that the optimal short-wavelength band edge is positioned just below the emission peak of Red305, say, between 560-580 nm (see Figure 4). However, due to the dependence of the reflection on the angle of incidence, the optimal short-wavelength band edge is red-shifted to 632 nm. An FSC (l=23.7 cm, d=1 mm) with an optimized TCM shows a gain in power of 14% compared to one without a TCM. As far as the cost-per-unit-of-power is concerned, a TCM should therefore add no more than 14% to the costs.

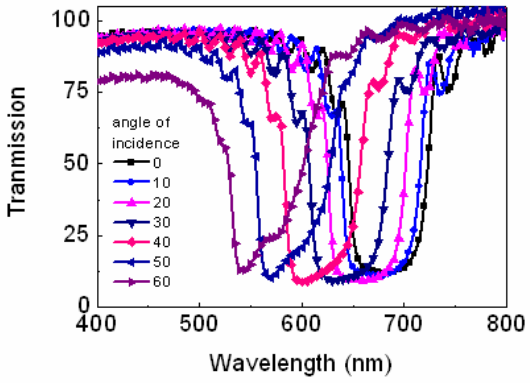

Figure 15 Measured transmission spectrum of a cholesteric mirror.

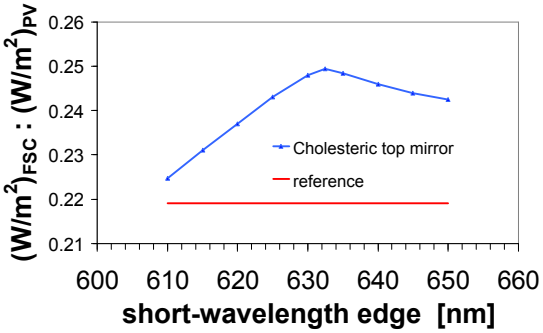

Figure 16 The relative power density as a function of the short-wavelength edge of the reflection band of the cholesteric top mirror. The red line represents the case without a cholesteric top mirror.

6 CONCLUSION

A parameter study has been performed for a Fluorescent Solar Concentrator (FSC) in which length and thickness of a square plate have been varied as well as the dye concentrations of CRS040 and Red305, and the type of bottom mirror. The computations were performed with a Monte-Carlo ray-trace program. A simple cost model was developed in which the polymer plate-to-PV cell cost per unit area ratio C_{PP}[€/m^2]/C_{PV}[€/m^2] was the key parameter. When C_{PP}[€/m^2]/C_{PV}[€/m^2]=1/15 the FSC can generate power at a cost price in €/W that is only 35% of that of conventional PV. In that case, the power of the FSC is 21% compared to conventional PV with the same size. When C_{PP}[€/m^2]/C_{PV}[€/m^2] =1/5 the €/W price of an FSC is as high as that of conventional PV. However, in that case the FSC power is only 22% of that of conventional PV and therefore one would always prefer the latter.

A target function for multiobjective optimization (cost and power) was introduced. This shows that, if one departs from an FSC with minimum cost-per-unit-of-power [€/W] one could increase the power with 3% at the expensive of only 1% increase in €/W, illustrating that optimization is a subjective choice of finding the right balance of objectives.

An additional study was performed to assess the performance gain if device parameters could be improved. Improvements in refractive index, Stokes shift, back ground absorption and the dye's quantum efficiency can yield an efficiency improvement up to 46%. Optimization of a cholesteric mirror leads to an efficiency increase of 14%, in a relative sense.

7 ACKNOWLEDGEMENT

This work has been supported in part by the European Commission as part of the Framework 6 integrated project FULLSPECTRUM (contract SES6-CT-2003-502620).

We greatly acknowledge Michael Debye from the Technical University of Eindhoven for providing us with the optical constants of the cholesteric mirror.

8 REFEERENCES

[1] M.A. Green, "Solar Cells. Operating Principles, Technology and System Applications.", ISBN 0 85823 580 3, (1998).

[2] Kennedy et al, 2007. "Modelling the effect of device geometry on concentration ratios of quantum dot solar concentrators", ISES Solar World Congress, Beijing, China.

[3] A.R. Burgers, L.H. Slooff, R. Kinderman and J.A.M. van Roosmalen, "Modelling of luminescent concentrators by ray-tracing", 20th EC Photovoltaic Solar Energy Conference, Barcelona, p. 394-397, 2005.

[4] A. Hübner, A.G. Aberle and R. Hezel, "Novel cost-effective bifacial solar cells with 19.4% front and 18.1% rear efficiency", Applied Physics Letter **70** (8), 24 February 1997.

[5] Hitachi, http://www.hitachi.com.au/pr-Bifacial-Solar-Cell.seo.

[6] L.H. Slooff, A.R. Burgers, E.E. Bende and M.G. Debye, "The luminescent solar concentrator: a parameter study towards maximum efficiency.", Proceedings of SPIE (2008), Vol. 7002.

[7] A. Zastrow, „Physikalische Analyse der Energievelustmechanismen im Fluoreszenzkollektor", Ph.D. Thesis (1981).

[8] L.H. Slooff, internal report of Framework 6 integrated project FULLSPECTRUM (contract SES6-CT-2003-502620).

[9] W.G.J.H.M van Sark et al., "Luminescent Solar Concentrators – A review of recent results", submitted to Optics Express (July, 2008).

A APPENDIX

A.1 The cost

For an FSC the area costs, C_{FSC}[€/m^2], are composed of the polymer plate and the PV-cells attached to one or more sides. In case of an infinite grid of square FSCs, each unit-cell FSC has two PV-cells on average. Therefore, the relative cost, i.e. compared with conventional PV, reads:

$$C_r = \frac{C_{FSC}[€/m^2]}{C_{PV}[€/m^2]} = \frac{(A_{top}[m^2]C_{PP}[€/m^2]+2A_{side}[m^2]C_{PV}[€/m^2])/A_{top}[m^2]}{C_{PV}[€/m^2]} = \frac{C_{PP}[€/m^2]}{C_{PV}[€/m^2]} + \frac{2d}{l}. \quad (4)$$

Here, A_{side} is the area of the PV-cell attached to one side of polymer plate, A_{top} is the top area of the square polymer plate, C_{PP}/C_{PV} denotes the area cost fraction, where C_{PP} is the area cost of the polymer plate and C_{PV} is the area cost of conventional PV. Furthermore, l is the length and d is the thickness of the FSC plate (in m).

A.2 Power density

We can calculate the power density of an FSC relative to that of a conventional photovoltaic cell. The power density of an FSC can be calculated as the power density of the PV cells attached to the four sides of the FSC times the area of the PV cells, divided by the top area of the polymer plate. This implies that the relative power density reads

$$P_r = \frac{p_{mp,PV-in-FSC}[\mathrm{Wm}^{-2}]A_{sides}[\mathrm{m}^2]/A_{top}[\mathrm{m}^2]}{p_{mp,PV}[\mathrm{Wm}^{-2}]} = \frac{p_{mp,PV-in-FSC}}{p_{mp,PV}}\frac{4d}{l}. \quad (5)$$

Here, $p_{mp,PV\text{-}in\text{-}FSC}$ is the electrical power density at the maximum power point of the PV cells attached to the four sides of the polymer plate illuminated with one sun, and p_{mp,pv_PV} is the same for a conventional PV system.

Elaborating the power-density fraction yields

$$P_r = \frac{\phi_{FSC-sides}}{\phi_{AM1.5G}} \cdot \frac{EQE_{emiss}}{EQE_{AM1.5G}} \cdot \frac{V_{oc,FSC}}{V_{oc,PV}} \cdot \frac{FF(v_{oc,FSC})}{FF(v_{oc,PV})} \cdot \frac{4d}{l} \qquad 6)$$

Here, *FF* is the fill factor that is a function which increases with increasing $v_{oc}=V_{oc}/(k_BT/q)$ [8], V_{oc} is the open-circuit voltage, ϕ is the photon flux in photons/m^2/s and EQE is the average external quantum efficiency of the PV cell. The suffix "emiss" refers to the spectrum that enters the PV cells at the sides of the FSC and that resembles the emission spectrum of the dye. The suffix AM1.5G refers to spectrum of the incident sunlight. Note that $q \cdot \Phi \cdot EQE$ is the short-circuit current density in Am^{-2}. If we insert the values for the successive ratios in eq. 7 of an FSC, optimized for lowest cost-per-unit-of-power, with dimensions l=0.25 m, d=0.01, with the max. Red305 concentration, no CRS040 yellow and a Lambertian bottom mirror with gap, the relative power becomes

$$P_r = 6.5 \times 1.74 \times 1.1 \times 1.01 \times 0.017 = 0.21 \qquad 7)$$

The first ratio is the optical concentration factor, which of course represents the basic concept of an FSC. The second ratio is composed of a numerator that equals unity, implying a one-on-one photon-to-electron conversion for the PV-cells at the FSC sides, and a denominator of 0.57. Due to the high concentration factor the photon intensity is high at the PV cells in the FSC. Consequently, the electric current density is higher compared to that of conventional PV. Since the open-circuit voltage scales linearly with the current density (Shockley), the V_{oc}-ratio is about 1.1. A higher V_{oc} on its turn results in a higher fill factor. This leads to FF-ratio of 1.01. The last term represents the reciprocal of the geometric gain and ultimately brings the total multiplication of all ratios down to 0.21. This implies that the power of an FSC yields only 21% of that of conventional PV with the same area. Thus, the efficiency of an FSC is 21% of that of conventional PV.